Journal of Oceanography, Vol. 62, pp. 293 to 301, 2006

Evaluation of Marine Surface Winds Observed by SeaWinds and AMSR on ADEOS-II

NAOTO EBUCHI*

Institute of Low Temperature Science, Hokkaido University, Kita-ku, Sapporo 060-0819, Japan

(Received 28 May 2005; in revised form 5 August 2005; accepted 5 August 2005)

Marine surface winds observed by two microwave sensors, SeaWinds and Advanced Microwave Scanning Radiometer (AMSR), on the Advanced Earth Observing Satellite-II (ADEOS-II) are evaluated by comparison with off-shore moored buoy observations. The wind speed and direction observed by SeaWinds are in good agreement with buoy data with root-mean-squared (rms) differences of approximately 1 m s^{-1} and 20°, respectively. No systematic biases depending on wind speed or cross-track wind vector cell location are discernible. The effects of oceanographic and atmospheric environments on the scatterometry are negligible. Though the wind speed observed by AMSR also showed agreement with buoy observations with rms difference of 1.27 m s^{-1}, the AMSR wind speed is systematically lower than the buoy data for wind speeds lower than 5 m s^{-1}. The AMSR wind seems to have a discontinuous trend relative to the buoy data at wind speeds of 5–6 m s^{-1}. Similar results have been obtained in an intercomparison of wind speeds globally observed by SeaWinds and AMSR on the same orbits. A global wind speed histogram of the AMSR wind shows skewed features in comparison with those of SeaWinds and European Centre for Medium-range Weather Forecasts (ECMWF) analyses.

Keywords:
· ADEOS-II,
· SeaWinds,
· AMSR,
· marine surface wind,
· remote sensing.

1. Introduction

The Advanced Earth Observing Satellite-II (ADEOS-II) was launched by the National Space Development Agency of Japan (NASDA) on 14 December 2002, into an 802.9-km, near-polar, sun-synchronous orbit at an inclination angle of 98.7°. The mission carries five sensors including SeaWinds and Advanced Microwave Scanning Radiometer (AMSR), that measure near-surface winds under all weather and cloud conditions over the global oceans.

SeaWinds is a microwave scatterometer that measures wind speed and directions over the ocean surface. It uses a rotating dish antenna with two pencil beams that sweep in a circular pattern at incidence angles of 46° (H-pol) and 52° (V-pol). The antenna radiates microwave pulses at a frequency of 13.4 GHz across broad regions of the Earth's surface. The instrument can measure vector winds over a swath of 1800 km with a nominal spatial resolution of 25 km. Daily coverage is about 92% of the global ice-free oceans. SeaWinds was also carried by the QuikSCAT satellite launched in June 1999. Ebuchi *et al*. (2002) reported that the wind speed and direction observed by SeaWinds on QuikSCAT are in good agreement with offshore buoy observations, with root-mean-squared (rms) differences of 1 m s^{-1} for wind speed and 23° for wind direction.

AMSR is a multi-frequency, dual-polarized microwave radiometer that measures microwave emissions from the Earth's surface and atmosphere. It measures scalar wind speed over the oceans together with various physical parameters of the ocean surface and atmosphere including sea surface temperature, integrated water vapor, liquid water content, and precipitation. AMSR has eight frequency channels (6.925, 10.65, 18.7, 23.8, 36.5, 50.3, 52.8, and 89.0 GHz) with dual polarization. Conical scanning is employed to observe the Earth's surface with a constant incidence angle of 55°. Multi-frequency measurement is accomplished with an array of primary horns. The offset-parabolic antenna has a diameter of 2 m and is the largest spaceborne microwave radiometer antenna. The typical sampling interval is 10 km and the swath of the observation is approximately 1450 km.

Marine surface winds observed by spaceborne microwave sensors over the global oceans with high spatial resolution and frequent temporal sampling are utilized in

* E-mail address: ebuchi@lowtem.hokudai.ac.jp

various fields of meteorology, oceanography, and climate studies to investigate such topics as ocean surface waves, wind-driven ocean circulations and air-sea fluxes of momentum, heat, water vapor, and gasses (e.g., reviews by Liu, 2002, and Katsaros *et al*., 2002). Surface vector wind and wind stress fields derived from scatterometer observations are applied to drive ocean circulation models on various scales and are also assimilated into global numerical weather prediction models. However, microwave scatterometers and radiometers do not directly measure the marine surface wind but instead measure the electromagnetic radiation backscattered or emitted from the sea surface. Surface winds are then estimated through empirical relationships between the backscatter cross sections or brightness temperatures and 10-m neutral equivalent winds (Liu and Tang, 1996). Validation of the observed winds is therefore necessary to evaluate the quality of the wind data and to assess the error structure. Numerous validation studies have been carried out by comparing winds derived from microwave scatterometers and radiometers with in-situ observations by buoys and vessels (e.g., Jones *et al*., 1982; Wentz *et al*., 1982; Bentamy *et al*., 1994; Wentz, 1997, Freilich and Dunbar, 1999; Masuko *et al*., 2000; Ebuchi *et al*., 2002; and their references).

In this paper, wind vectors observed by SeaWinds and wind speed observed by AMSR are evaluated by comparison with data from the National Data Buoy Center (NDBC), Tropical Atmosphere Ocean/Triangle Trans-Ocean Buoy Network (TAO/TRITON) and Pilot Research Moored Array in the Tropical Atlantic (PIRATA) buoys deployed in the Atlantic and Pacific Oceans and Gulf of Mexico. Furthermore, wind speeds observed by SeaWinds and AMSR on the same satellite orbits are compared with each other in order to assess the consistency of the measurements. Section 2 briefly describes the data utilized in this study. Section 3 presents comparisons of wind vectors derived from SeaWinds and buoy observations, while Section 4 provides comparisons of scalar wind speed derived from AMSR with buoy data. Intercomparison of SeaWinds and AMSR wind speeds is described in Section 5. A brief summary is given in Section 6.

2. Data

2.1 SeaWinds

This study uses the SeaWinds Science Data Product, Level 2B (JPL, 2002), which was processed and distributed by the National Aeronautics and Space Administration (NASA)/Jet Propulsion Laboratory (JPL) Physical Oceanography Distributed Active Archive Center (PO.DAAC). The wind data were produced using a Maximum-Likelihood Estimator (MLE; Long and Mendel, 1991) with the QSCAT-1 geophysical model function and a median filter ambiguity removal algorithm (Shaffer *et al*., 1991) with the Numerical Weather Product (NWP) initialization. The spatial resolution of the wind data is 25 km and the reference level of the wind vectors is 10 m. The Multidimensional Histogram (MUDH) Rain Flag (Huddleston and Stiles, 2000) was applied to indicate the presence of rain. All the flagged data were discarded, including data with rain flag. Data observed in a period from 10 April 2003 to 24 October 2003 were used.

2.2 AMSR

The study uses the AMSR Level-2 Standard Product/Sea Surface Wind (version 3), processed and distributed by the Japan Aerospace Exploration Agency (JAXA). The AMSR standard algorithm developed by Shibata (2002) is used to derive the wind speed from the brightness temperatures. The first version (version 1) was released to users in December 2003. Based on evaluations of the version 1 product, the wind retrieval algorithm was refined and the entire data product was reprocessed using the new algorithm. The version 3 data product is now available to users (the version 2 product was not released to the public). The wind speed is retrieved from the brightness temperatures at frequencies of 36.5, 10.65, and 6.925 GHz (Shibata, 2002). The instantaneous field of views (IFOVs) of these channels are 8×14, 27×46, and 40×70 km, respectively. The spatial sampling interval of the wind speed contained in the Level-2 Standard Product is approximately 10 km. The version 3 product over the period from 10 April 2003 to 24 October 2003 is analyzed here.

2.3 Ocean buoys

For comparison with the SeaWinds and AMSR wind data, buoy observations from 34 NDBC, 48 TAO/TRITON, and 7 PIRATA buoys were collected. Only those buoys located offshore and in deep water were selected. The locations of the buoys are shown in Fig. 1. Details of the NDBC and TAO buoys, instruments, and stations were described by Meindl and Hamilton (1992) and McPhaden (1995), respectively. The PIRATA buoys are identical to the TAO buoys. High temporal sampling data with an interval of 10 min. are utilized. The wind speed measured by the buoys at various heights above the sea surface was converted to equivalent neutral wind speed at a height of 10 m using the method proposed by Liu and Tang (1996).

The SeaWinds and AMSR wind data and buoy observations were collocated in time and space by choosing SeaWinds/AMSR wind observation cells closest to the buoy locations in space and the buoy data closest to the SeaWinds/AMSR observations in time. Temporal difference and spatial separation between the SeaWinds/AMSR and buoy observations were restricted to less than 10 min. and 12.5 km, respectively.

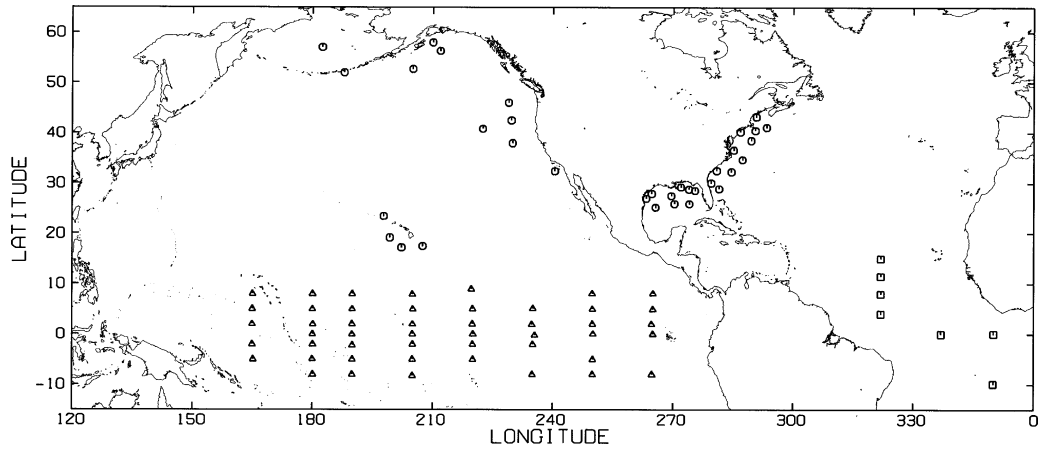

Fig. 1. Locations of the NDBC (circles), TAO/TRITON (triangles), and PIRATA (squares) buoys used in this study.

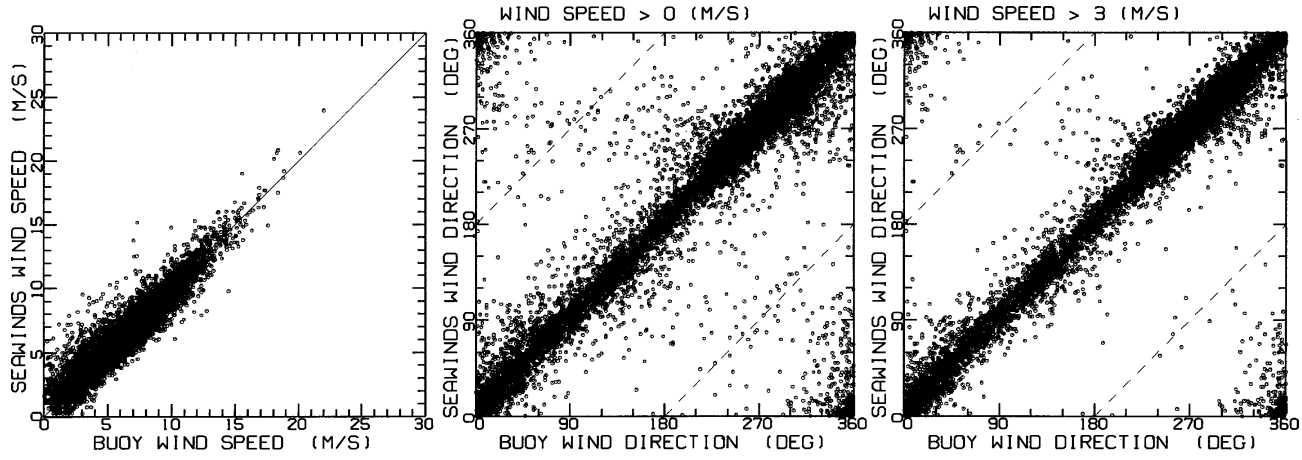

Fig. 2. Comparison of wind speed (left) and direction (middle for data of all the wind speed ranges, and right for data of wind speed greater than 3 m s^{-1}) observed by SeaWinds with buoy data.

3. Comparison of Wind Speed and Direction Observed by SeaWinds with Buoy Data

Figure 2 shows a comparison of wind speed and direction observed by SeaWinds with the buoy data. Statistical values of the comparison are summarized in Table 1. In general, both the wind speed and direction derived by SeaWinds on ADEOS-II are in good agreement with buoy observations. No systematic biases in the wind speed and direction are discernible.

In the comparison of wind speed, the bias is negligible, and the rms difference is approximately 1 m s^{-1}, which is much smaller than the mission requirement of 2 m s^{-1} (JPL, 2002). In terms of wind direction, the rms difference is greater than 25°. If one considers data of buoy wind speed higher than 3 m s^{-1}, the rms difference is considerably reduced to about 20°, indicating that the accuracy of the SeaWinds-derived wind direction at low wind speed range is worse than that at moderate to high wind speed ranges. This result also indicates that the mission requirement for the wind direction measurement, which is less than 20° in the wind speed range from 3 to 20 m s^{-1}, is almost satisfied. These results are similar to comparisons of wind vectors observed by SeaWinds on QuikSCAT with buoy data reported by Ebuchi *et al.* (2002).

Figure 3 shows the dependences of wind speed and direction residuals (SeaWinds–buoy) on the buoy wind speed. The wind speed residual (a) is close to zero and shows no systematic dependence on the buoy wind speed over the whole wind ranges, except at low wind speeds, where artificial positive bias due to the asymmetrical distribution of data points (Freilich, 1997) is discernible. In terms of the residual of wind direction (b), the standard deviation increases at low wind range, corresponding to

Table 1. Statistical values of the comparison of wind speed and direction observed by SeaWinds with buoy data.

	Number of data points	Bias	Rms difference	Correlation coefficient
Wind speed (m/s)	10754	–0.04	0.93	0.937
Wind direction (°)				
(Buoy wind speed > 0 m/s)	10670	3.3	29.2	0.962
(Buoy wind speed > 3 m/s)	9301	3.0	20.7	0.980
(Buoy wind speed > 5 m/s)	6938	2.7	15.3	0.988

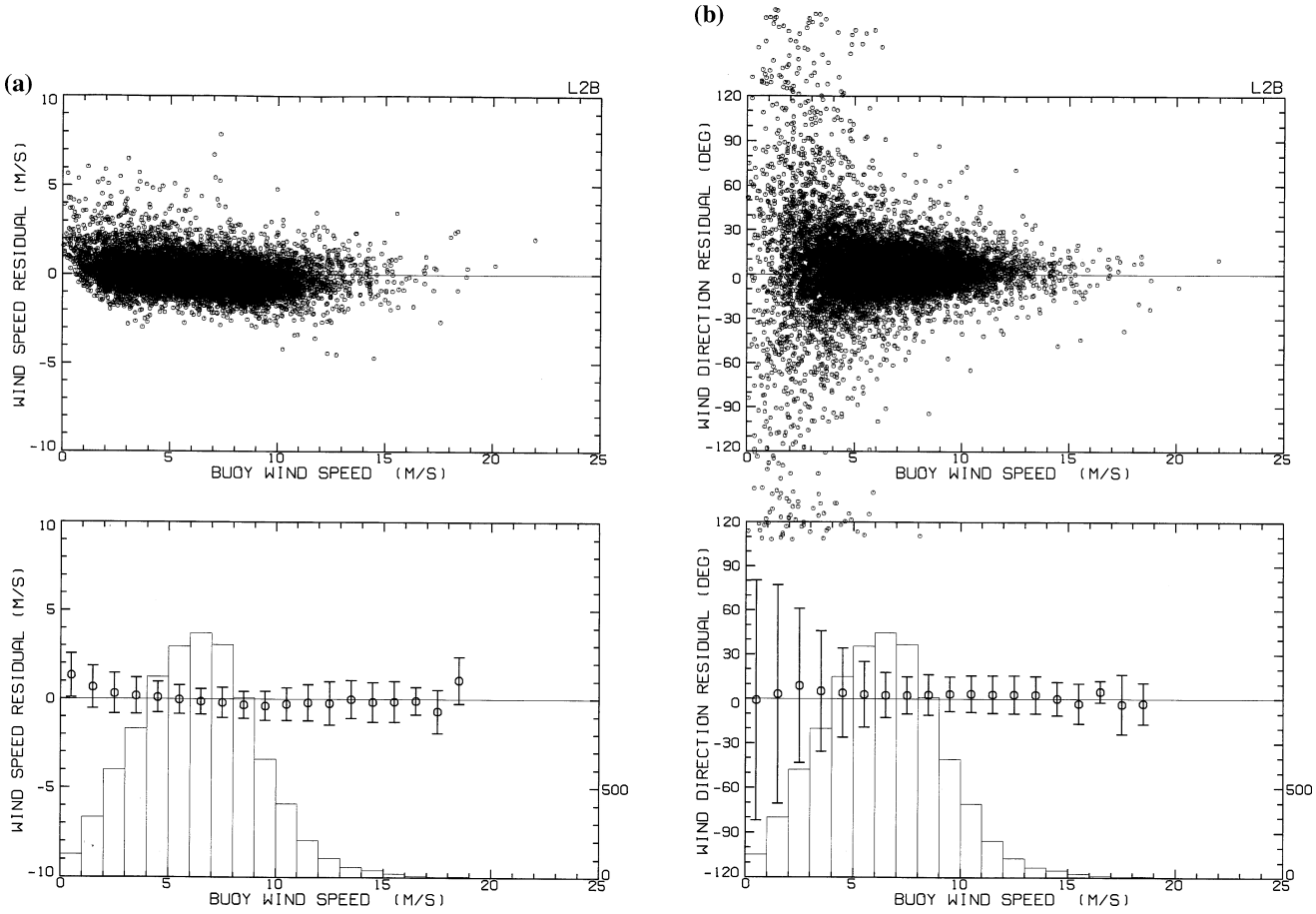

Fig. 3. Dependence of residuals (SeaWinds–buoy) of (a) the wind speed and (b) direction on the buoy wind speed.

the result in Table 1 and indicating that wind directions at low wind speeds are less accurate. This inaccuracy probably results from the low upwind/crosswind modulation of the microwave backscattering property from the sea surface. It is also possible that the ambiguity removal technique is less accurate at low wind speeds.

Dependences of the residuals on the cross-track location of wind vector cells, which corresponds to combination of azimuth angles of the scatterometer beams, are shown in Fig. 4. For outer cells (those toward cells 1 and 76), the scatterometer beams are aligned in the cross-track directions, while for inner cells (those toward cells 38 and 39), the beams are aligned with the spacecraft flight direction (JPL, 2002). The standard deviations of both wind speed (a) and direction (b) increase slightly towards the inner and outer cells.

In order to assess the influence of atmospheric and oceanic conditions on the scatterometry, correlations between the wind speed residual (SeaWinds–buoy) with various atmospheric and oceanic parameters observed by the buoys are calculated and shown in Table 2. Only the data of buoy wind speed ranging from 9 to 12 m s^{-1} are

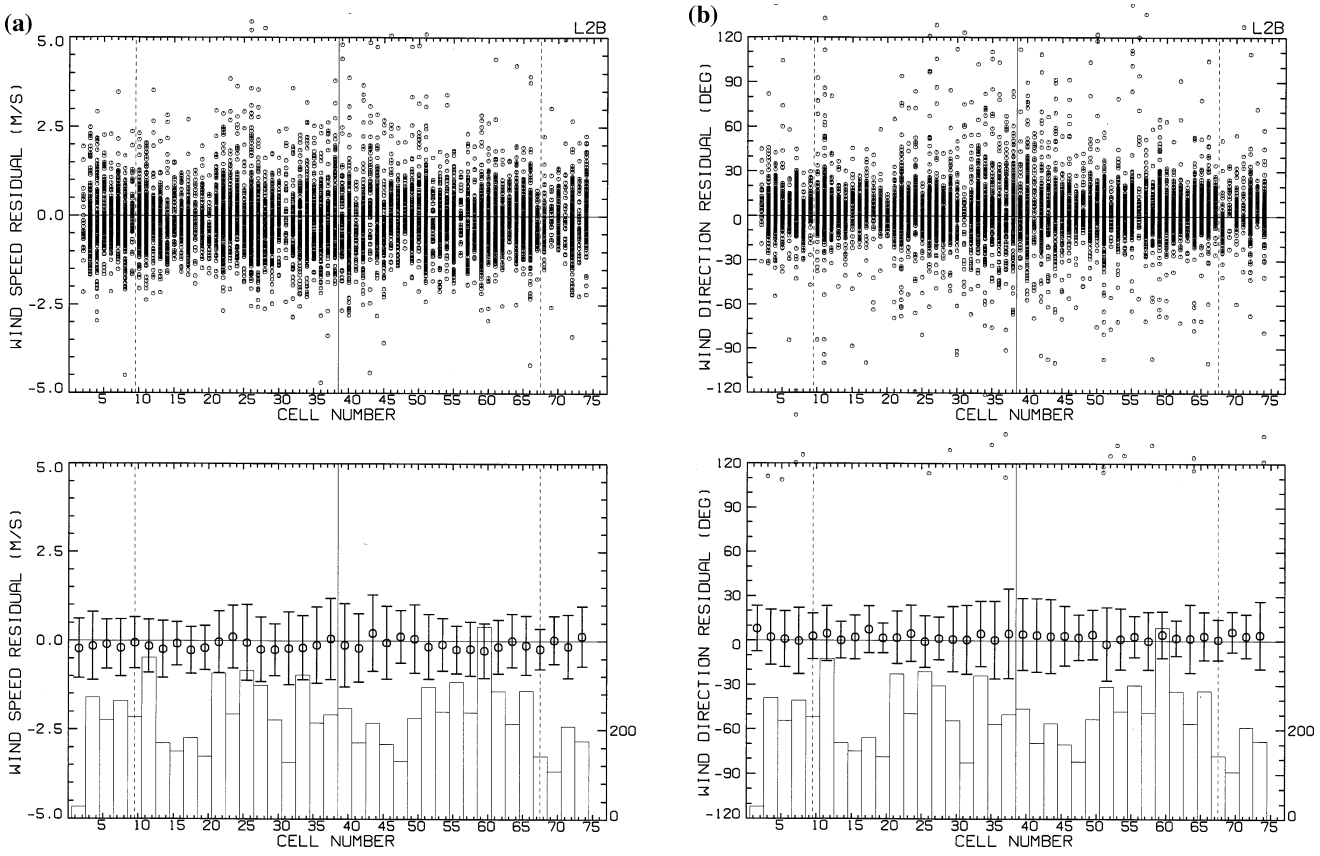

Fig. 4. Dependence of residuals (SeaWinds–buoy) of (a) the wind speed and (b) direction on cross-track location of wind vector cells.

Table 2. Correlation of the wind speed residuals (SeaWinds–buoy) with the atmospheric and oceanic parameters for buoy wind speed in the range from 9 to 12 m s^{-1}.

	Number of data points	Correlation coefficient	Slope
Sea surface temperature	1387	–0.127	–0.015 (m s^{-1}/K)
Air temperature	1387	–0.122	–0.014 (m s^{-1}/K)
Air-sea temperature difference	1387	–0.024	–0.019 (m s^{-1}/K)
Specific humidity	743	–0.096	–0.026 (m s^{-1}/g m^{-3})
Significant wave height	973	+0.143	+0.111 (m s^{-1}/m)
Inverse wave age	970	–0.123	–0.615 (m s^{-1})
Buoy wind speed	1387	+0.078	+0.090 (m s^{-1}/m s^{-1})

used. The number of data points differs for each parameter, as some of the NDBC buoys do not measure the humidity, and the TAO and PIRATA buoys do not measure the wave parameters. In the last line, the correlation of the residual with the buoy wind speed is shown to confirm that the residual has no dependence on the wind speed itself and the correlation obtained is not due to a spurious effect of wind speed dependence of the residual.

In Table 2, the wind speed residual shows poor correlations with the parameters representing the thermal condition of the sea surface, such as the sea surface temperature, and air-sea temperature difference. Furthermore, the significant wave height and inverse wave age, which represent the sea state, exhibit weak correlations with the wind speed residual. Although the correlation coefficients listed in Table 2 are statistically significant, exceeding the 99% confidence limit (approximately 0.08), the influence of the environments represented by these param-

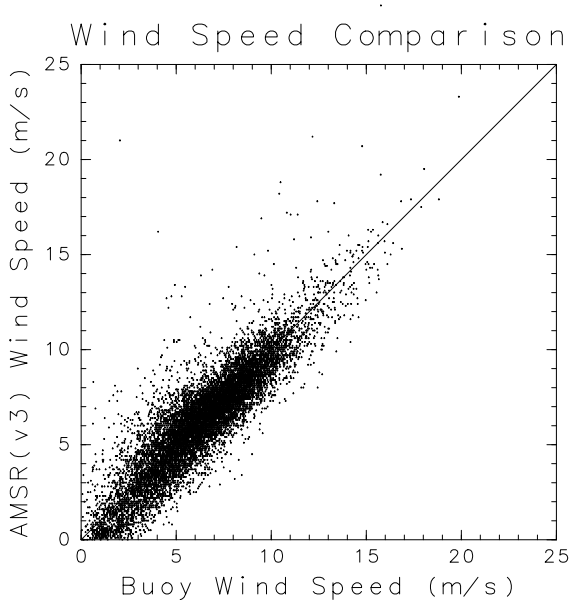

Fig. 5. Comparison of wind speed observed by AMSR with buoy data.

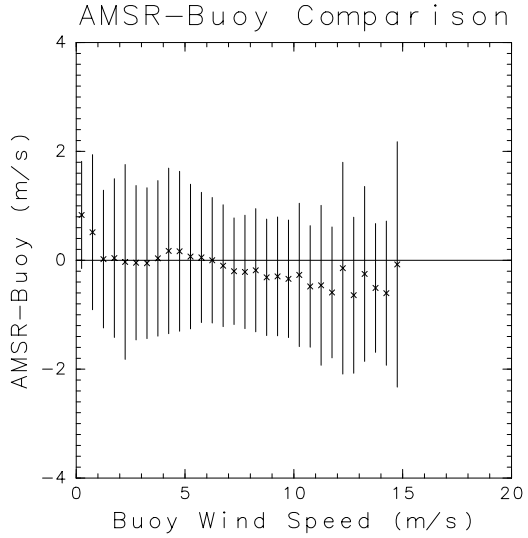

Fig. 6. Dependence of wind speed residual (AMSR–buoy) on the buoy wind speed.

eters is considered to be small. For example, an increase of 10°C in the sea surface temperature under the same wind conditions may cause a decrease of wind speed of only 0.15 m s^{-1}. This feature does not vary with the wind range within a range of wind speed from 3 to 15 m s^{-1}, where the wind speed residual does not depend on the wind speed itself.

The results presented in Table 2 indicate that the influence of the thermal condition of the sea surface and the sea state have negligible influence on the Ku-band radar backscattering. This conclusion is consistent with results from the NSCAT Ku-band scatterometer on ADEOS (Ebuchi *et al.*, 1998) and SeaWinds on QuikSCAT (Ebuchi *et al.*, 2002), although several previous studies have reported that the microwave backscattering from the sea surface may be influenced by the sea surface temperature (e.g., Donelan and Pierson, 1987; Ebuchi *et al.*, 1996; Graber *et al.*, 1996; Ebuchi, 1997), the stability of the atmospheric boundary layer (e.g., Keller *et al.*, 1985; Colton *et al.*, 1995), and the sea state (e.g., Keller *et al.*, 1985; Li *et al.*, 1989; Ebuchi *et al.*, 1996; Graber *et al.*, 1996). Errors in the scatterometer and buoy observations and temporal and spatial separations of the observations in the comparison might smear the influences of the thermal conditions and sea state. Limitation of the ranges of the atmospheric and oceanic parameters due to the buoy locations and relatively short data period (7 months) may also result in the reduction of the correlations.

The stability of the atmospheric boundary layer above the sea surface is considered to have two possible effects, as discussed by Ebuchi *et al.* (2002). Under the same wind speed at a height above the sea surface (e.g., 10 m), the wind stress (or momentum transfer from the air to water), which generates small-scale waves contributing to the radar backscatter, varies with the atmospheric stability. Under the same wind stress acting on the sea surface, generation of the small-scale waves may also be affected by the stability. The former effect is already taken into account in the present comparison, since the buoy wind speed is converted to the 10-m neutral equivalent wind, which has a one-to-one relationship with the wind stress. Some of the previous studies used the wind speed measured by an anemometer at a height above the sea surface instead of the neutral equivalent wind and reported the stability dependence of the microwave backscattering from the sea surface. It is suggested that the latter effect is smaller, since it does not appear in the correlation listed in Table 2.

4. Comparison of Wind Speed Observed by AMSR with Buoy Data

Figure 5 shows a comparison of AMSR wind speed with buoy observations. The bias (AMSR–buoy) and rms difference are –0.07 m s^{-1} and 1.27 m s^{-1}, respectively. These values are comparable to or slightly larger than those for the SeaWinds wind speed listed in Table 1, and might be considered acceptable. It should be pointed out, however, that the AMSR wind is systematically lower than the buoy data at wind speed lower than 5 m s^{-1}. Moreover, the AMSR wind speed seems to have a discontinuous trend relative to the buoy data at wind speed of 5–6 m s^{-1}.

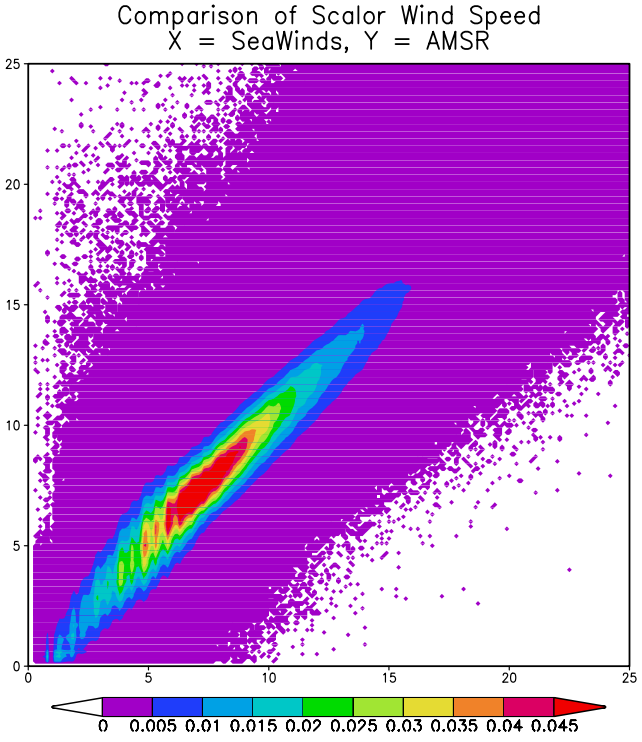

Fig. 7. Comparison of wind speeds observed by AMSR and SeaWinds. Horizontal and vertical axes are the SeaWinds and AMSR wind speeds in m s^{-1}. Number density of data points (%) in bins of 0.1 × 0.1 m s^{-1} is shown by contours.

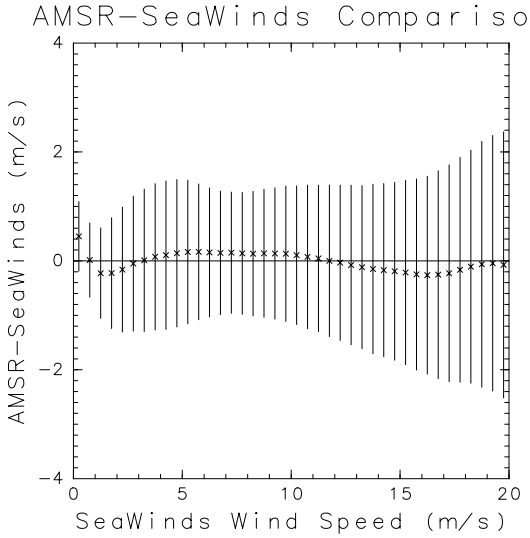

Fig. 8. Dependence of wind speed residual (AMSR–SeaWinds) on SeaWinds wind speed.

Residuals of wind speed (AMSR–buoy) are averaged in bins of 0.5 m s^{-1} of buoy wind speed. The result is shown in Fig. 6 with standard deviations. As discussed by Freilich (1997), the positive bias at very low wind speed (<3 m s^{-1}) is considered to be an artificial effect due to the asymmetric distribution of data points about the one-to-one line and does not indicate systematic overestimation of the wind speed. This effect also masks the underestimation of the wind speed by AMSR at very low wind ranges (wind speed lower than 5 m s^{-1}) shown in Fig. 5. At wind speeds higher than 10 m s^{-1} the AMSR wind speed is systematically lower than the buoy observations.

5. Intercomparison of Wind Speed Observed by SeaWinds and AMSR

Wind data globally observed by SeaWinds and AMSR along identical satellite orbits were collocated by wind cell-to-cell. All the flagged data were discarded, including rain flagged data. Only data observed in latitudes between 65°S and 65°N are used to avoid contamination by sea ice, which was not detected by AMSR and SeaWinds. The number of collocated data points is approximately 61 million.

Figure 7 shows the comparison of wind speeds observed by AMSR and SeaWinds. Number density of the data points in bins of 0.1 × 0.1 m s^{-1} is shown by contours. The bias (AMSR–SeaWinds) and rms difference are 0.06 m s^{-1} and 1.24 m s^{-1}, respectively, indicating that wind speeds observed by the two sensors are generally in good agreement. It is shown, however, that the trend changes discontinuously around 5–6 m s^{-1}, as shown in Fig. 5. In the wind speed range lower than 5 m s^{-1}, the wind speed derived from AMSR is systematically lower than that from SeaWinds. The large size of the AMSR–SeaWinds collocated data set exhibits the discontinuous trend more clearly than in Fig. 5. According to Shibata (personal communication), the discontinuous trend is considered to be caused by errors in the correction for the wind direction dependence of the brightness temperatures, which applied in the wind speed range higher than about 5 m s^{-1}.

Residuals of wind speed (AMSR–SeaWinds) are averaged in bins of 0.5 m s^{-1} of SeaWinds wind speed and plotted in Fig. 8 as in Fig. 6. Figure 8 shows a similar dependence of the wind speed bias on wind speed to that in Fig. 6, although underestimation of wind speed at higher wind ranges (wind speed higher than 7 m s^{-1}) is reduced compared to Fig. 6. The underestimation of wind speed by AMSR in low wind speed ranges appears around 2 m s^{-1}. In general, however, the wind speed difference between AMSR and SeaWinds is within a magnitude of 0.2 m s^{-1}.

Histograms of wind speed over the global oceans are calculated from all the wind speed data in latitudes from 65°S to 65°N and for the period of 7 months from April

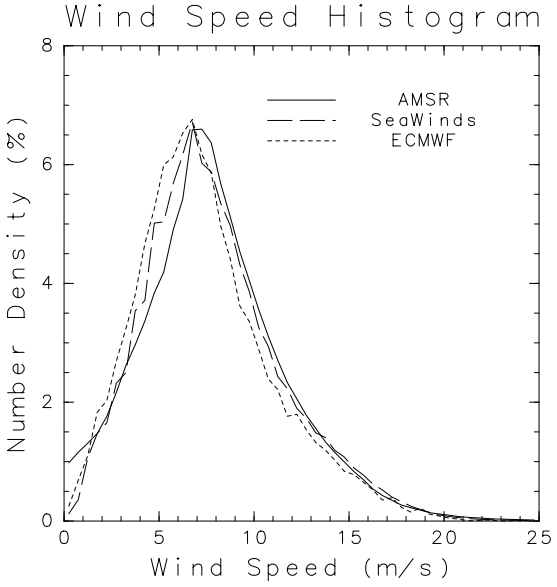

Fig. 9. Global wind seed histograms for AMSR, SeaWinds, and ECMWF wind data.

to October 2003. Comparison of the global wind speed histograms is shown in Fig. 9. For reference, the histogram calculated from the European Centre for Medium-range Weather Forecasts (ECMWF) analysis (2.5° × 2.5°, 12 hour intervals) in the same period is also shown in the figure. Although the histograms of SeaWinds and ECMWF are in good agreement, the histogram of AMSR wind shows slightly different features from them. The histogram of AMSR wind contains more data at very low wind speed (lower than 1.5 m s^{-1}) and fewer data in a wind speed range from 3 to 6 m s^{-1}. The systematic under/overestimations in the AMSR wind shown in Figs. 5, 6, 7, and 8 might cause convergence or divergence of data distribution and result in the skewed histogram.

6. Summary

Marine surface winds observed by two microwave sensors, SeaWinds and AMSR, on ADEOS-II are evaluated by comparison with off-shore NDBC, TAO/TRITON and PIRATA buoy observations. Only the buoys located offshore were selected. Time difference and spatial separation between the SeaWinds or AMSR and buoy observations were limited to less than 10 min. and 12.5 km, respectively. Wind speed measured by the buoys at various heights above the sea surface was converted to the 10-m neutral equivalent wind by using the method proposed by Liu and Tang (1996).

The wind speed and direction observed by SeaWinds are in good agreement with buoy data and satisfy the mission requirement. The rms difference of wind speed is about 1 m s^{-1}. No systematic biases depending on wind speed or cross-tack wind vector cell location are discernible. The rms difference of wind direction is about 20° for data of wind speed higher than 3 m s^{-1}. The effects of oceanographic and atmospheric conditions on the scatterometry were also assessed using the collocated data set. No significant dependences of wind speed residual on the sea surface temperature, the air-sea temperature difference, or the sea state are discernible.

The wind speed observed by AMSR also exhibits an agreement with buoy observations in general with rms difference of 1.27 m s^{-1}, which is slightly larger than that for the SeaWinds wind speed. However, the AMSR wind speed is systematically lower than the buoy data for wind speed lower than 5 m s^{-1}. The AMSR wind seems to have a discontinuous trend relative to the buoy data at wind speeds of 5–6 m s^{-1}, which might be caused by errors in the correction for the wind direction dependence of the brightness temperatures.

Wind speeds observed by AMSR and SeaWinds were compared with each other in order to assess the consistency of the measurements. A collocated data set was produced from global wind measurements by the two sensors on the same satellite orbits for the period of 7 months from April to October 2003. Approximately 61 million collocated data points were obtained. The AMSR wind speed is systematically lower than the SeaWinds wind speed in the wind speed range lower than 5 m s^{-1}. There is also a slight discontinuity at wind speeds of 5–6 m s^{-1} in the comparisons with SeaWinds data. These differences are consistent with the results of the comparison with buoy observations. An intercomparison of wind speed histograms calculated from the global 7-months observations revealed that the AMSR winds exhibit a skewed histogram in comparison with those of SeaWinds and ECMWF analysis. These results suggest that further refinements of the AMSR wind retrieval algorithm are required. Base on the results of this study, it can be concluded that the SeaWinds currently provides wind data with higher quality than AMSR.

Acknowledgements

The author gratefully acknowledges funding support from the Japan Aerospace Exploration Agency (JAXA). This study was also supported in part by the Category 7 of MEXT RR2002 Project for Sustainable Coexistence of Human, Nature and the Earth. He also appreciates Dr. Akira Shibata, JAXA, for his discussion and information concerning the AMSR wind retrieval algorithms and data processing. The National Data Buoy Center (NDBC) and the Tropical Ocean Atmosphere (TAO) Project Office provided the buoy data. The SeaWinds and AMSR data products used in this study were obtained from the NASA/JPL PO-DAAC and JAXA, respectively. The author expresses his sincere thanks to these data providers. Some

of the figures in this paper were produced by GFD-DENNOU Library.

References

Bentamy, A., Y. Quilfen, P. Queffeulou and A. Cavanie (1994): Calibration of the ERS-1 scatterometer C-band model. Tech. Rep., IFREMER/Brest, DRO/OS-94-01, Brest, France, 72 pp.

Colton, M. C., W. J. Plant, W. C. Keller and G. L. Geernaert (1995): Tower-based measurements of normalized radar cross-section from Lake Ontario: Evidence of wind stress dependence. *J. Geophys. Res.*, **100**, 8791–8813.

Donelan, M. A. and W. J. Pierson (1987): Radar scattering and equilibrium ranges in wind-generated waves with application to scatterometry. *J. Geophys. Res.*, **92**, 4971–5029.

Ebuchi, N. (1997): Sea surface temperature dependence of C-band radar cross sections observed by ERS-1/AMI scatterometer. *J. Adv. Mar. Sci. Tech. Soc.*, **3**, 157–168.

Ebuchi, N., H. C. Graber and R. Vakkayil (1996): Evaluation of ERS-1 scatterometer winds with wind and wave ocean buoy observations. Tech. Rep. CAOS, Tohoku University, CAOS 96-1, p. 1–69.

Ebuchi, N., H. C. Graber, A. Bentamy and A. Mukaida (1998): Evaluation of NSCAT winds with ocean buoy observations. *Proc. PORSEC'98*, Qingdao, China, p. 396–400.

Ebuchi, N., H. C. Graber and M. J. Caruso (2002): Evaluation of wind vectors observed by QuikSCAT/SeaWinds using ocean buoy data. *J. Atmos. Oceanic Tech.*, **19**, 2049–2062.

Freilich, M. H. (1997): Validation of vector magnitude datasets: Effects of random component errors. *J. Atmos. Oceanic Tech.*, **17**, 695–703.

Freilich, M. H. and R. S. Dunbar (1999): The accuracy of the NSCAT-1 vector winds: Comparison with NDBC buoys. *J. Geophys. Res.*, **104**, 11,231–11,246.

Graber, H. C., N. Ebuchi and R. Vakkayil (1996): Evaluation of ERS-1 scatterometer winds with wind and wave ocean buoy observations. Tech. Rep. RSMAS, University of Miami, RSMAS 96-003, p. 1–69.

Huddleston, J. N. and B. W. Stiles (2000): Multidimensional Histogram (MUDH) Rain Flag Product Description (version 3.0). Jet Propul. Lab., Pasadena, CA, p. 8 (this document can be obtained from http://podaac.jpl.nasa.gov/quikscat/qscat-doc.html).

Jones, W. L., L. C. Schroeder, D. H. Boggs, E. M. Bracalante, R. A. Brown, G. J. Dome, W. J. Pierson and F. J. Wentz (1982): The relationship between wind vector and normalized radar cross section used to derive SEASAT-A satellite scatterometer winds. *J. Geophys. Res.*, **87**, 3318–3336.

JPL (2002): SeaWinds Science Data Product User's Manual (version 1.0), Jet Propulsion Laboratoty Publ. D-21551, Pasadena, CA, p. 122 (this document can be obtained from http://podaac.jpl.nasa.gov/seawinds).

Katsaros, K. B., P. W. Vachon, W. T. Liu and P. G. Black (2002): Microwave remote sensing of tropical cyclones from space. *J. Oceanogr.*, **58**, 137–151.

Keller, W. C., W. J. Pierson and D. E. Weissman (1985): The dependence of X band microwave sea return on atmospheric stability and sea state. *J. Geophys. Res.*, **90**, 1019–1029.

Li, F., W. Large, W. Shaw, E. J. Walsh and K. Davidson (1989): Ocean radar backscattering relationship with near-surface winds: A case study during FASINEX. *J. Phys. Oceanogr.*, **19**, 342–353.

Liu, W. T. (2002): Progress in scatterometer application. *J. Oceanogr.*, **58**, 121–136.

Liu, W. T. and W. Q. Tang (1996): Equivalent neutral wind. JPL Publ. 96-19, Jet Propul. Lab., Pasadena, Calif., p. 8 (this document can be obtained from http://airsea-www.jpl.nasa.gov/data).

Long, D. E. and J. M. Mendel (1991): Identifiability in wind estimation from scatterometer measurements. *IEEE Trans. Geosci. Remote Sens.*, **GE-29**, 268–276.

Masuko, H., K. Arai, N. Ebuchi, M. Konda, M. Kubota, K. Kutsuwada, T. Manabe, A. Mukaida, T. Nakazawa, A. Nomura, A. Shibata and Y. Tahara (2000): Evaluation of vector winds observed by NSCAT in the seas around Japan. *J. Oceanogr.*, **56**, 495–505.

McPhaden, M. J. (1995): The Tropical Atmosphere Ocean array is completed. *Bull. Amer. Meteorol. Soc.*, **76**, 739–741.

Meindl, E. A. and G. D. Hamilton (1992): Programs of the National Data Buoy Center. *Bull. Amer. Meteorol. Soc.*, **73**, 985–993.

Shaffer, S. J., R. S. Dunbar, S. V. Hisao and D. G. Long (1991): A median-filter-based ambiguity removal algorithm for NSCAT. *IEEE Trans. Geosci. Remote Sens.*, **GE-29**, 167–174.

Shibata, A. (2002): AMSR/AMSR-E sea surface wind speed algorithm. *EORC Bull.*, **9**, 94 pp. (this document can be obtained from http://sharaku.eorc.jaxa.jp/AMSR/doc/index.htm).

Wentz, F. J. (1997): A well-calibrated ocean algorithm for special sensor microwave/imager. *J. Geophys. Res.*, **102**, 8703–8718.

Wentz, F. J., V. J. Cardone and L. S. Fedor (1982): Intercomparison of wind speeds inferred by the SASS, Altimeter, and SMMR. *J. Geophys. Res.*, **87**, 3378–3384.